J|A|C|S
ARTICLES
Published on Web 02/06/2004

Dynamics of Competitive Reactions: Endothermic Proton Transfer and Exothermic Substitution

Jianhua Ren[1] and John I. Brauman*

Contribution from the Department of Chemistry, Stanford University, Stanford, California 94305-5080

Received January 6, 2003; Revised Manuscript Received November 21, 2003; E-mail: brauman@stanford.edu

Abstract: Dynamics of an endothermic proton-transfer reaction, F^- with dimethyl sulfoxide, and an endothermic proton-transfer reaction with a competing exothermic substitution (S_N2) channel, F^- with borane−methyl sulfide complex, were investigated using a Fourier transform ion cyclotron resonance mass spectrometer (FT-ICR) and kinetic modeling. The two proton-transfer reactions have slightly positive and a small negative overall free energy changes, respectively. Energy-dependent rate constants were measured as a function of F^- ion translational energy, and the resulting kinetics were modeled with the RRKM (Rice−Ramsperger−Kassel−Marcus) theory. The observed rate constants for the proton-transfer reactions of F^- with dimethyl sulfoxide and with borane−methyl sulfide complex are identical, with a value of 0.17×10^{-9} cm^3 molecule^{-1} s^{-1}; for the S_N2 reaction, $k = 0.90 \times 10^{-9}$ cm^3 molecule^{-1} s^{-1} at 350 K. Both proton-transfer reactions have positive entropy changes in the forward direction and show positive energy dependences. The competing S_N2 reaction exhibits negative energy dependence and becomes less important at higher energies. The changes of the observed rate constants agree with RRKM theory predictions for a few kcal/mol of additional kinetic energy. The dynamic change of the branching ratio for the competing proton transfer and the substitution reactions results from the competition between the microscopic rate constants associated with each channel.

Introduction

A variety of endothermic ion−molecule reactions have been observed and studied with mass spectrometry.[2−6] Most endothermic reactions proceed slowly in the gas phase, although some endothermic reactions are observed to be fast.[7−10] These fast reactions often involve large entropy gains in the forward direction and hence have negative overall free energy changes. Such reactions are referred to as "entropy-driven" reactions.[11,12] A series of entropy-driven reactions, charge transfer (eq 1a)[13] and proton transfer (eq 1b),[12,14] for example, have been observed and studied with ion cyclotron resonance and high-pressure mass spectrometers at variable temperatures. Equilibrium constants were observed in favor of product formation, and the forward reactions were found to occur much faster than the enthalpy term ($\Delta H°$) would allow. More interestingly, some of the reactions appeared to reach collision rates at higher temperatures. These results lead to conclusions that fast endothermic reactions are best characterized by a barrierless single well potential energy surface and the kinetics are determined by the free energy changes.[12,13]

A large positive entropy change can significantly reduce the free energy for a reaction, especially at higher temperatures ($\Delta G° = \Delta H° - T\Delta S°$). When the magnitude of $T\Delta S°$ is large enough, $\Delta G°$ and $\Delta H°$ can have opposite signs, that is, $\Delta H° > 0$ and $\Delta G° < 0$. A positive entropy change in a reaction can occur for many reasons; the most familiar is an increase in translational entropy in a reaction because of a larger number of particles on the product side.[7,8,15] Other cases involve increases in vibrational and rotational entropy, for example, on the release of a hydrogen bonding interaction in the product with ring opening,[9,16−18] a change in conformation, or an increase in rotational degrees of freedom, from an atomic ion to a diatomic molecule.[12] All of these reactions are characterized by favorable entropy changes. The observed rate constants, however, are macroscopic quantities, an integration of energy-dependent microscopic counterparts weighted according to the energy distribution.

(1) Current address: University of the Pacific.
(2) Viggiano, A. A.; Morris, R. A. *J. Phys. Chem.* **1996**, *100*, 19227−19240.
(3) Kronberg, J. E.; Stone, J. A. *Int. J. Mass Spectrom. Ion Phys.* **1977**, *24*, 373−388.
(4) Ausloos, P.; Lias, S. G. *Int. J. Mass Spectrom. Ion Processes* **1984**, *58*, 165−180.
(5) Su, T.; Kevan, L.; Tiernan, T. O. *J. Chem. Phys.* **1971**, *54*, 4871−4880.
(6) Angel, L. A.; Garcia, S. P.; Ervin, K. M. *J. Am. Chem. Soc.* **2002**, *124*, 336−345.
(7) Aschi, M.; Chiavarino, B.; Crestoni, M. E.; Fornarini, S. *J. Phys. Chem.* **1996**, *100*, 19859−19863.
(8) Feng, W. Y.; Iraqi, M.; Lifshitz, C. *J. Phys. Chem.* **1993**, *97*, 3510−3514.
(9) Gorman, G. S.; Amster, I. J. *Org. Mass Spectrom.* **1993**, *28*, 1602−1607.
(10) Williams, T. L.; Adams, N. G.; Babcock, L. M. *Int. J. Mass Spectrom. Ion Processes* **1998**, *172*, 149−159.
(11) Henchman, M. *NATO ASI Ser., Ser. C* **1987**, *193*, 381−383.
(12) Meot-Ner, M. *J. Phys. Chem.* **1991**, *95*, 6580−6585.
(13) Sieck, L. W.; Meot-Ner, M. *J. Phys. Chem.* **1982**, *86*, 3646−3650.
(14) Meot-Ner, M. *J. Am. Chem. Soc.* **1989**, *111*, 2830−2834.
(15) King, G. K.; Maricq, M. M.; Bierbaum, V. M.; DePuy, C. H. *J. Am. Chem. Soc.* **1981**, *103*, 7133−7140.
(16) Yamdagni, R.; Kebarle, P. *J. Am. Chem. Soc.* **1973**, *95*, 3504−3510.
(17) Crowder, C. A.; Bartmess, J. E. *J. Am. Soc. Mass Spectrom.* **1993**, *4*, 723−726.
(18) Meot-Ner, M.; Hamlet, P.; Hunter, E. P.; Field, F. H. *J. Am. Chem. Soc.* **1980**, *102*, 6393−6399.

10.1021/ja030006z CCC: $27.50

Entropy effects have been observed as an important factor affecting dynamics of gas-phase reactions involving a double well potential energy surface, such as a substitution reaction (S_N2, eq 1c).[19] The efficiency of an S_N2 reaction is a result of the competition between a complex dissociating to reactants, which has a positive entropy change, and the conversion to products, which can have a lower energy but is less favorable entropically.[20]

$$A^+ + B \rightarrow A + B^+ \quad (1a)$$

$$A^- + BH \rightarrow AH + B^- \quad (1b)$$

$$X^- + RY \rightarrow XR + Y^- \quad (1c)$$

Dynamic analysis of isoergic proton-transfer reactions ($A^- + AH$) suggests that the observed kinetics are influenced by several dynamic factors involved in the association and the dissociation of the ion−molecule complex.[21] A study of the dissociation of a proton-transfer intermediate complex $[(NC)_2CH_2{\cdot}Cl]^-$ at two widely separated energy regimes (about 30 kcal/mol) indicated that the branching ratio of $(NC)_2CH^-$ versus Cl^- is qualitatively consistent with a statistical RRKM (Rice−Ramsperger−Kassel−Marcus) model. In this study, the higher energy proton-transfer intermediate was generated via an S_N2 reaction, $CN^- + NCCH_2Cl$, and the proton-transfer channels were found to compete with the S_N2 channel.

In this study, we chose a reaction that has an endothermic proton-transfer channel competing with an exothermic S_N2 reaction. As a comparison, we also studied an endothermic proton-transfer reaction independently. We investigated the dynamics of these reactions by measuring rate constants as a function of reactant ion translational energy, and we model the reaction kinetics with statistical RRKM theory.

Experimental Section

Experiments. Experiments were carried out in an IonSpec OMEGA Fourier transform ion cyclotron resonance mass spectrometer (FT-ICR) equipped with an ion kinetic energy controller.[22,23] Briefly, the instrument is operated at a 0.6 T magnetic field with a background pressure of 3×10^{-9} Torr. The temperature in the ICR cell was estimated to be 350 K.[24] Neutral reagents were added to the vacuum chamber through variable leak valves. The pressure of the neutral reagents was measured with a Varian ionization gauge calibrated against a MKS Baratron capacitance manometer. The primary ions were generated by electron impact, and the unwanted ions were removed by using ejection pulses. Impulse excitation was used to excite the ions prior to detection. On-resonance excitation of the selected ion was achieved using an ion kinetic energy controller.[23] The ion kinetic energy controller supplies 180° phase-shifting radio frequency (rf) with variable voltage to the selected ion, so that the ion can be alternately accelerated and decelerated. On average, the ion kinetic energy is higher than the thermal energy. The average center-of-mass kinetic energy was determined from trajectory calculations of ions undergoing reversible rf acceleration.[25]

All chemicals were purchased from Aldrich and were used without further purification. Multiple freeze−pump−thaw cycles were applied to all of the gaseous and liquid chemicals prior to introduction into the vacuum chamber. The reactant ion, F^-, was generated by electron impact on NF_3. The neutral reagents, dimethyl sulfoxide (**1**) and borane−methyl sulfide complex (**2**), were introduced into the vacuum chamber through leak valves. The pressure of the neutral reagents was in the range of $(2-5) \times 10^{-7}$ Torr. To determine rate constants at different translational energies of F^-, the intensities of F^- were measured as a function of time while an on-resonance rf signal (in the range of 1−2 V/m)[26] was applied to the F^- ion. Data were fit to eq 2 (where C is a constant and n is the number density, in molecule cm^{-3}, of the neutral reactant). Control experiments show that the relative ion loss as well as the intensity of the irradiated ions are not affected significantly by this procedure. The absolute uncertainty of the experimental results was estimated to be about 10%. Mass balance was examined by measuring the total ion intensity (reactant + product) with acceleration of F^- and by comparing the total ion intensity with that measured without the acceleration signal.[23] For H/D exchange experiments, neutral CH_3OD was introduced into the ICR cell to react with hydrogen-containing ions. If H/D exchange occurs, new peak(s) with one mass unit higher would show up. The numbers of new peaks represent the numbers of H/D exchanges.[27,28]

$$\ln[F^-] = n{\cdot}k{\cdot}t + C \quad (2)$$

Quantum Calculations.[29] The structures and vibrational frequencies for the neutral molecules, ions, and ion−molecule complexes were calculated using the B3LYP/6-31G(d) and the MP2/6-31+G(d) methods. The transition state was located on the B3LYP potential energy surface using the QST3 method. True energy minima and the saddle point were confirmed by frequency analysis and by viewing the motion of the structure corresponding to each vibrational mode. For all of the structures at the energy minima, no imaginary frequency was found. For the transition state structure, one imaginary frequency was found. Relative energies were obtained at the MP2/6-311+G(2d,p)//B3LYP/6-31G(d), B3LYP/6-311+G(3df,2p)//MP2/6-31+G(d), and G2MP2 levels of theory. The calculated results were compared with the available experimental data.

Statistical Modeling. The reaction kinetics were modeled with the RRKM program, HYDRA.[30] A detailed statistical model and the modeling procedure are described in a previously published paper.[31] Briefly, the RRKM theory predicted rate constant can be described as the collision rate constant (k_{coll}) multiplied by the macroscopic reaction efficiency (Φ),[32] eq 3. The macroscopic efficiency is the integration

(19) Shaik, S. S.; Schlegel, H. B.; Wolfe, S. *Theoretical Aspects of Physical Organic Chemistry. The SN2 mechanism*; Wiley: New York, 1992.
(20) Craig, S. L.; Zhong, M.; Brauman, J. I. *J. Am. Chem. Soc.* **1999**, *121*, 11790−11797.
(21) Lim, K. F.; Brauman, J. I. *J. Chem. Phys.* **1991**, *94*, 7164−7180.
(22) Wilbur, J. L. Ph.D. Dissertation, Stanford University, 1993.
(23) Boering, K. A.; Rolfe, J.; Brauman, J. I. *Int. J. Mass Spectrom. Ion Processes* **1992**, *117*, 357−386.
(24) Han, C. C.; Brauman, J. I. *J. Am. Chem. Soc.* **1989**, *111*, 6491−6496.
(25) Craig, S. L.; Brauman, J. I. *J. Phys. Chem. A* **1997**, *101*, 4745−4752.
(26) Ren, J.; Brauman, J. I. *J. Phys. Chem. A* **2002**, *106*, 3804−3813.
(27) DePuy, C. H.; Bierbaum, V. M.; King, G. K.; Shapiro, R. H. *J. Am. Chem. Soc.* **1978**, *100*, 2921−2922.
(28) Stewart, J. H.; Shapiro, R. H.; DePuy, C. H.; Bierbaum, V. M. *J. Am. Chem. Soc.* **1977**, *99*, 7650−7653.
(29) Frisch, M. J.; Trucks, G. W.; Schlegel, H. B.; Scuseria, G. E.; Robb, M. A.; Cheeseman, J. R.; Zakrzewski, V. G.; Montgomery, J. A.; Stratmann, R. E.; Burant, J. C.; Dapprich, S.; Millam, J. M.; Daniels, A. D.; Kudin, K. N.; Strain, M. C.; Farkas, O.; Tomasi, J.; Barone, V.; Cossi, M.; Cammi, R.; Mennucci, B.; Pomelli, C.; Adamo, C.; Clifford, S.; Ochterski, J.; Petersson, G. A.; Ayala, P. Y.; Cui, Q.; Morokuma, K.; Malick, D. K.; Rabuck, A. D.; Raghavachari, K.; Foresman, J. B.; Cioslowski, J.; Ortiz, J. V.; Baboul, A. G.; Stefanov, B. B.; Liu, G.; Liashenko, A.; Piskorz, P.; Komaromi, I.; Gomperts, R.; Martin, R. L.; Fox, D. J.; Keith, T.; Al-Laham, M. A.; Peng, C. Y.; Nanayakkara, A.; Challacombe, M.; Gill, P. M. W.; Johnson, B.; Chen, W.; Wong, M. W.; Andres, J. L.; Gonzalez, C.; Head-Gordon, M.; Replogle, E. S.; Pople, J. A. *Gaussian 98*; Gaussian, Inc.: Pittsburgh, PA, 1998.
(30) Wladkowski, B. D.; Lim, K. F.; Brauman, J. I. *HYDRA: Calculation of ion−molecule reaction rate coefficients using variational transition state theory*; 1991, unpublished.
(31) Wladkowski, B. D.; Lim, K. F.; Allen, W. D.; Brauman, J. I. *J. Am. Chem. Soc.* **1992**, *114*, 9136−9153.
(32) Moylan, C. R.; Brauman, J. I. *Adv. Classical Trajectory Methods* **1994**, *2*, 95−114.

Table 1. Enthalpy and Free Energy at 298 K, in kcal/mol[34]

reaction	$\Delta H°$	$\Delta G°$
$(CH_3)_2SO \rightarrow CH_3SOCH_2^- + H^+$	373.5[a]	366.4[a]
$(CH_3)_2SBH_3 \rightarrow CH_3S(BH_3)CH_2^- + H^+$	372.5[b]	364.3[b]
$HF \rightarrow F^- + H^+$	371.3[c]	365.5[c]
$(CH_3)_2SO + F^- \rightarrow CH_3SOCH_2^- + HF$	+2.2[d]	+0.9[d]
$(CH_3)_2SBH_3 + F^- \rightarrow CH_3S(BH_3)CH_2^- + HF$	+1.2[d]	−1.2[d]

[a] Reference 40 (value altered from reference due to change in acidity scale).[34] [b] Reference 41. [c] Reference 42. [d] Values derived from the previous three reactions in Table 1.

of the microscopic counterparts weighted according to the thermal equilibrium energy and angular momentum distribution of the ion−molecule complex. RRKM theory is incorporated into the microscopic efficiency calculation. The corresponding collision rate constants are calculated using the Su trajectory model, in which the relative kinetic energy of the system is a variable.[33] At thermal condition (350 K), the theoretically predicted efficiency is fit to the experimentally observed efficiency, eq 4. This can be achieved by adjusting the barrier height (the energy difference between the transition state and the intermediate complex) of the product formation channel. To model a system at increased translational energy, the added translational energy is assumed to be incorporated into the internal modes of the reactant complex. Therefore, the average total energy of the system is equal to the average thermal energy (350 K) of the reactants plus the center-of-mass collision energy. The temperature is replaced with an effective temperature corresponding to a temperature at which the collision complex has a Boltzmann distribution of total internal energy, and the theoretical efficiency is calculated with increasing effective temperature.

When F^- ion was undergoing collision with a neutral molecule, the kinetic energy added to the F^- was assumed to be incorporated into the internal energy of the system. Therefore, the average total energy of the reaction system is a combination of the center-of-mass collision energy and the average thermal internal energy (350 K) of the reactants. The temperature of the system is replaced with an effective temperature.

$$k_{RRKM} = k_{coll} \cdot \Phi \tag{3}$$

$$\Phi = k_{obs}/k_{coll} \tag{4}$$

The proton-transfer reactions of F^- with both **1** and **2** were assumed to have a single well potential energy surface, and the S_N2 reaction of F^- with **2** was assumed to have a conventional double well potential energy surface. The transition state of the proton-transfer channel was treated as product-like with one 2D-rotor associated with H−F formation (the 20 cm^{-1} of the rotational constant for H−F was treated as an active rotational mode for energy redistribution in the proton-transfer transition state). The relative energies of relevant species on the potential energy surfaces were taken from energy calculations, and the vibrational frequencies and rotational constants were obtained from the frequency calculations at the B3LYP/6-31G(d) level.

Results

Experimental Results. We studied reactions of F^- with dimethyl sulfoxide (**1**) and borane−methyl sulfide complex (**2**). Thermochemical quantities of these reactions can be derived from thermochemical cycles, involving the gas-phase acidity of **1**, **2**, and HF (Table 1). Proton transfer (PT) from **1** to F^- (eq 5) is endothermic by 2.2 kcal/mol, while the free energy change for this reaction is 0.9 kcal/mol at 298 K (0.7 kcal/mol at 350 K). The reaction of F^- with **2** proceeds via two competing channels, proton transfer (eq 6a) and S_N2 (eq 6b). The proton-transfer reaction is endothermic by 1.2 kcal/mol, but with a free energy change of −1.2 kcal/mol at 298 K (−1.6 kcal/mol at 350 K). The S_N2 reaction is exothermic by 19.8 kcal/mol.[34] We measured rate constants as a function of increasing F^- translational energy, and we modeled the kinetic results with RRKM theory.

Table 2. Experimental Rate Constants, Collision Rate Constants, and Efficiencies Obtained at 350 K

reactants	channel	k_{obs} (10^{-9} cm^3 $molecule^{-1}$ s^{-1})	k_{coll} (10^{-9} cm^3 $molecule^{-1}$ s^{-1})	Φ
$(CH_3)_2SO + F^-$	PT	0.17	4.8	0.035
$(CH_3)_2SBH_3 + F^-$	total	1.1	5.0	0.21
	S_N2	0.90		0.18
	PT	0.17		0.034

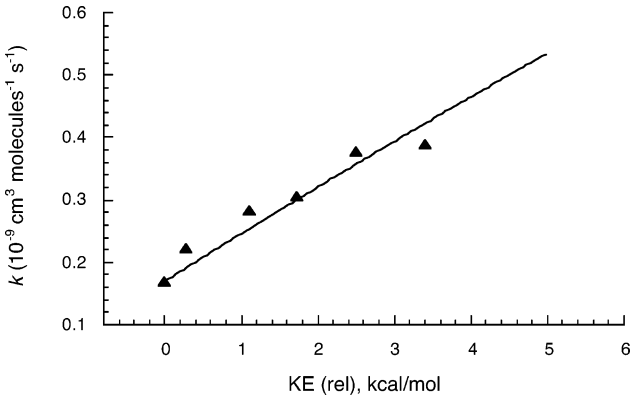

Figure 1. Experimental (▲) and RRKM (−) rate constants versus relative kinetic energies for the reaction of $CH_3SOCH_3 + F^-$.

$$\underset{\mathbf{1}}{CH_3SOCH_3} + F^- \rightarrow CH_3SOCH_2^- + HF \tag{5}$$

$$\underset{\mathbf{2}}{CH_3S(BH_3)CH_3} + F^- \rightarrow CH_3S(BH_3)CH_2^- + HF \tag{6a}$$

$$\rightarrow CH_3SBH_3^- + CH_3F \tag{6b}$$

The reaction of F^- with **1** produced only one ionic product, $CH_3SOCH_2^-$. The proton-transfer rate constant was determined by measuring the decay of F^- as a function of time, and a value of 0.17×10^{-9} cm^3 $molecule^{-1}$ s^{-1} was obtained at 350 K. The collision rate constant was calculated to be 4.8×10^{-9} cm^3 $molecule^{-1}$ s^{-1} by using the Su trajectory model,[33] giving an efficiency of 0.035 (Table 2). When F^- was accelerated with an on-resonance radio frequency, the reaction rate was observed to increase as a function of F^- translational energy. The results are plotted in Figure 1.

The reaction of F^- with **2** generated two product ions, $CH_3SBH_3^-$ (S_N2, *m*/*z* 61) and $CH_3S(BH_3)CH_2^-$ (PT, *m*/*z* 75), in a ratio of 5:1 at 350 K. Borane transfer from **2** to $CH_3SBH_3^-$ would give $CH_3SBH_3BH_3^-$ (*m*/*z* 75), which would overlap with the peak of $CH_3S(BH_3)CH_2^-$. Boron isotope patterns show the percentage of $CH_3SBH_3BH_3^-$ (two borons) as compared to $CH_3S(BH_3)CH_2^-$ (one boron). We examined the formation of

(33) Su, T. *J. Chem. Phys.* **1994**, *100*, 4703.

(34) *NIST Chemistry Webbook, NIST Standard Reference Database Number 69*; National Institue of Standards and Technology; March, 2003.

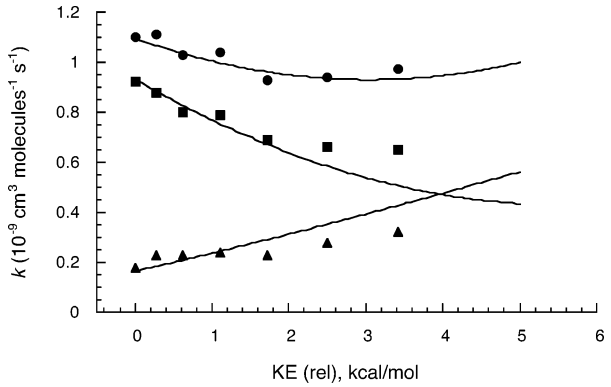

Figure 2. Experimental (● total, ■ S_N2, ▲ PT) and RRKM (−) rate constants versus relative kinetic energies for the reaction of $CH_3S(BH_3)CH_3 + F^-$.

$CH_3SBH_3BH_3^-$ as a function of reaction time and found that the intensity of $CH_3SBH_3BH_3^-$ was less than 5% within 1 s. We collected all kinetic data at 0.6 s with negligible $CH_3SBH_3BH_3^-$. Furthermore, hydrogen−deuterium exchange reactions between CH_3OD and the ion with *m*/*z* 75 showed a maximum of five H/D exchanges, suggesting that the ion with *m*/*z* 75 corresponded to the structure of $CH_3S(BH_3)CH_2^-$.[35] The overall rate constant for reaction 6 was determined by measuring the decay of F^- as a function of time, and a value of 1.1×10^{-9} cm^3 molecule^{-1} s^{-1} was obtained. The collision rate constant was calculated to be 5.0×10^{-9} cm^3 molecule^{-1} s^{-1}, giving an overall efficiency of 0.21. Combined with the product branching ratio of 5:1 (S_N2 to PT), we obtained rate constants for the S_N2 and the proton transfer of 0.90×10^{-9} and 0.17×10^{-9} cm^3 molecule^{-1} s^{-1}, and efficiencies of 0.18 and 0.034 at 350 K, respectively (Table 2). As the F^- was accelerated, the overall rate constant was insensitive to the energy change. The rate constant of the S_N2 reaction is decreased, and the rate constant of the proton transfer is increased. The results are plotted in Figure 2.

Computational Results. To obtain vibrational frequencies for kinetic modeling and qualitative energetic information, we performed quantum calculations with Gaussian 98.[29] We optimized structures of the neutral molecules and intermediate complexes for the two reaction systems using the B3LYP/6-31G(d) method. Corresponding vibrational frequencies and rotational constants were evaluated at the same level of theory. For comparison, we also optimized structures using the MP2/6-31+G(d) method. The two methods give similar geometries for reactants and products, and slightly different bond lengths between F^- and the neutral moiety in intermediate complexes. Stable ion−molecule complexes were found for both reactions 5 and 6. In the complex of F^- with **1**, [(CH_3SOCH_3) F^-] (**3**), the distance between the F^- and the two methyl carbons was calculated to be 2.74 Å with B3LYP and 2.93 Å with MP2. Similarly, the MP2 method predicts a longer (by 0.2 Å) distance between the F^- and the two methyl carbons in the complex of F^- with **2**, [($CH_3S(BH_3)CH_3$) F^-] (**4**). In both complexes **3** and **4**, the F^- is apparently hydrogen bonded to one hydrogen on each of the two methyl groups. This type of nonlinear hydrogen bonding has also been found in the calculated structure of dimethyl sulfoxide−hydroxide complex.[36]

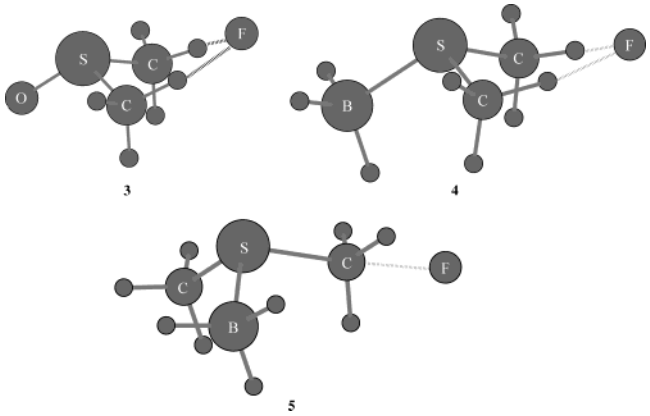

Relative energies for reaction 5 were calculated using the MP2/6-311+G(2d,p)//B3LYP/6-31G(d) and the B3LYP/6-311+G(3df,2p)//MP2/6-31+G(d) procedures. Complex **3** was calculated to be 28.2 kcal/mol (MP2/6-311+G(2d,p)//B3LYP/6-31G(d)) and 29.3 kcal/mol (B3LYP/6-311+G(3df,2p)//MP2/6-31+G(d)) below the separated reactants. A proton-transfer product complex, corresponding to the structure of [($CH_3SOCH_2^-$) HF], was calculated to have an energy about 12 kcal/mol higher than **3**. A search for a transition state between **3** and the product complex was unsuccessful at the B6LYP/6-31G(d) level, suggesting that the proton-transfer transition state structure is unstable. The proton-transfer products, $CH_3SOCH_2^- + HF$, were calculated to be 6.2 kcal/mol (MP2/6-311+G(2d,p)//B3LYP/6-31G(d)) and 6.4 kcal/mol (B3LYP/6-311+G(3df,2p)//MP2/6-31+G(d)) higher in energy than the reactants, $CH_3SOCH_3 + F^-$.

We calculated relative energies for reaction 6 at both the MP2/6-311+G(2d,p)//B3LYP/6-31G(d) and the G2MP2 levels of theory. The proton-transfer reaction 6a was calculated to be endothermic by 5.8 kcal/mol (MP2/6-311+G(2d,p)//B3LYP/6-31G(d)) and 4.4 kcal/mol (G2MP2), and the S_N2 reaction 6b was calculated to be exothermic by 24.4 kcal/mol (MP2/6-311+G(2d,p)//B3LYP/6-31G(d)) and 25.7 kcal/mol (G2MP2). Complex **4** was found to be 30.9 kcal/mol (MP2/6-311+G(2d,p)//B3LYP/6-31G(d)) and 31.5 kcal/mol (G2MP2) below the separated reactants. The proton-transfer product complex, [($CH_3S(BH_3)CH_2^-$) HF], was calculated to be about 10 kcal/mol above **4**, and the S_N2 product complex, [($CH_3SBH_3^-$) CH_3F], was calculated to be 1.6 kcal/mol below **4** at the MP2/6-311+G(2d,p)//B3LYP/6-31G(d) level. A S_N2 transition state, **5**, was located at 18.4 kcal/mol (MP2/6-311+G(2d,p)//B3LYP/6-31G(d)) above **4**. The geometry of the transition state has a normal S_N2 transition state structure, except that the methyl group has a slightly nonplanar geometry. Because the calculated energy of the transition state was not important for kinetic modeling, we did not perform further energetic calculations.

For the S_N2 reaction to reach transition state **5**, intermediate **4** has to rearrange to a formal S_N2 reactant complex with the F^- attached to the backside of the reaction center, the methyl carbon. This reactant complex is likely to have an energy between that of **4** and **5**. We performed an energy scan procedure

(35) Ren, J.; Workman, D. B.; Squires, R. R. *Angew. Chem., Int. Ed. Engl.* **1997**, *36*, 2230−2232.

(36) Burk, P.; Molder, U.; Koppel, I. A.; Rummel, A.; Trummal, A. *J. Phys. Chem.* **1996**, *100*, 16137−16140.

to locate the reactant complex, starting from **5** and ending with complex **4**. The potential energy falls smoothly, and no additional intermediate complex was found at the B3LYP/6-31G(d) level. The S_N2 reactant complex is probably located in a shallow well and is insensitive to this computational procedure. Apparently complex **4** serves as a common intermediate for both the proton transfer and the S_N2 reactions.

Statistical Modeling. The reaction of F^- with **1** (eq 5) was modeled with a single well potential energy surface with ion−molecule complex **3** associated with the well (Discussion section). Complex **3** can either dissociate back to the reactants (k_B) or give the proton-transfer products (k_{PT}). The entrance and the exit channels were assumed to have reactant-like and product-like transition states, respectively.[37] The efficiency for the overall reaction is described using eq 7. The efficiency of reaction 5 was measured to be 0.035 at 350 K. Statistical modeling gives the barrier height, the energy difference between the transition state and the complex, of the product channel to be 30.9 kcal/mol, corresponding to a 2.7 kcal/mol endothermicity for the overall proton-transfer reaction. By using the energetic quantities obtained at 350 K, we calculated a series of theoretical efficiencies at higher system energies (associated with increasing effective temperature). We also calculated the corresponding collision rate constants using the Su trajectory model. The collision rate constant decreases slowly as a function of increase in collision energy. With an additional 5 kcal/mol of kinetic energy, the collision rate constant decreases by 20%. Combining the efficiencies obtained with statistical modeling and the calculated collision rate constants, we obtained RRKM rate constants (eq 3) as a function of kinetic energy. The RRKM rate constants show positive energy dependence (Figure 1).

$$\Phi_{PT} = \frac{k_{PT}}{k_B + k_{PT}} \tag{7}$$

The reaction of F^- with **2** (eq 6) was modeled with two competing channels, the S_N2 and the proton transfer (PT). The S_N2 channel was treated as a double well, and the proton transfer was treated as a single well potential energy surface (Discussion section). The ion molecule complex **4** was assumed to be the common intermediate for the two channels. Because the S_N2 reaction is highly exothermic, the rate-determining step would be the crossing of the S_N2 central barrier. The efficiency for each exit channel is associated with the branching over the three pathways, dissociation back to the reactants (k_B), crossing the S_N2 central barrier (k_{SN2}), and formation of the proton-transfer products (k_{PT}). The efficiency for the S_N2 channel can be described using eq 8, and the efficiency for the proton-transfer channel can be described using eq 9.

$$\Phi_{SN2} = \frac{k_{SN2}}{k_B + k_{SN2} + k_{PT}} \tag{8}$$

$$\Phi_{PT} = \frac{k_{PT}}{k_B + k_{SN2} + k_{PT}} \tag{9}$$

The experimentally measured overall efficiency for reaction 6 is 0.21 at 350 K. The measured efficiency for the S_N2 reaction is 0.18, and that for the proton transfer is 0.034. Statistical modeling gives the central barrier height for the S_N2 channel as 23.9 kcal/mol, corresponding to 7 kcal/mol below the separated reactants. The modeling gives a barrier height for the proton-transfer channel of 33.7 kcal/mol, corresponding to 2.8 kcal/mol of endothermicity for the proton-transfer reaction. With increasing system energy (corresponding to increasing the effective temperature), the efficiency for the S_N2 channel is decreased, and the efficiency for the proton transfer increased. The corresponding RRKM rate constants at different system energies were obtained by multiplying the theoretical efficiencies by the calculated collision rate constants (eq 3). The S_N2 rate constants show negative energy dependence, and the proton transfer shows positive energy dependence (Figure 2).

Discussion

We have investigated the dynamics of endothermic proton-transfer reactions and the proton-transfer reaction with a competing S_N2 channel by measuring the rate constants as a function of reactant ion translational energy and modeling the kinetic results with RRKM theory. Proton transfer from **1** to F^- has a rate constant of 0.17×10^{-9} cm^3 molecule^{-1} s^{-1} and an efficiency of 0.035 at 350 K. The observed rate constant increases as the F^- translational energy is increased. The changes of the rate constants agree with RRKM theory predictions (Figure 1). The reaction of F^- with **2** has an overall rate constant of 1.1×10^{-9} cm^3 molecule^{-1} s^{-1} and an efficiency of 0.21 at 350 K. The proton transfer and the S_N2 channels have rate constants of 0.17×10^{-9} and 0.90×10^{-9} cm^3 molecule^{-1} s^{-1}, corresponding to efficiencies of 0.034 and 0.18, respectively. The overall rate constant is insensitive to energy change, while the proton-transfer channel shows positive energy dependence and the S_N2 channel shows negative energy dependence. The observe rate constants agree with RRKM theory predictions in the energy range examined, although theory predicts a larger change at higher energies (Figure 2).

The ion molecule complex **3** has a calculated association energy of about 28 kcal/mol. The strong binding between F^- and dimethyl sulfoxide is apparently a result of the hydrogen bonding between the F^- and the hydrogens on the two methyl groups in dimethyl sulfoxide in addition to an ion−dipole interaction.[31] Our calculations show that the corresponding proton-transfer product complex, [($CH_3SOCH_2^-$)HF], is higher than **3** by 12 kcal/mol, and is located in a shallow well. No transition state structure can be located between **3** and [($CH_3SOCH_2^-$)HF]. Complex **3** is likely a stable intermediate for the proton-transfer reaction. The energy profile for the reaction of F^- with **1** may well be represented using a single well potential energy surface with **3** associated with the well[32] (Figure 3). A single well potential energy surface has been employed to characterize a large number of fast proton-transfer and charge-transfer reactions, including a series of entropy-driven endothermic reactions.[12,38] Complex **3** can exit the well by either forming the proton-transfer products (the PT

(37) Moylan, C. R.; Brauman, J. I. *Annu. Rev. Phys. Chem.* **1983**, *34*, 187−215.
(38) Wilbur, J. L.; Wladkowski, B. D.; Brauman, J. I. *J. Am. Chem. Soc.* **1993**, *115*, 10823−10829.
(39) Bohme, D. K.; Mackay, G. I.; Schiff, H. I. *J. Phys. Chem.* **1980**, *84*, 4976−4986.
(40) Bartmess, J. E.; Scott, J. A.; McIver, R. T., Jr. *J. Am. Chem. Soc.* **1979**, *101*, 6046−6056.
(41) Ren, J.; Workman, D. B.; Squires, R. R. *J. Am. Chem. Soc.* **1998**, *120*, 10511−10522.

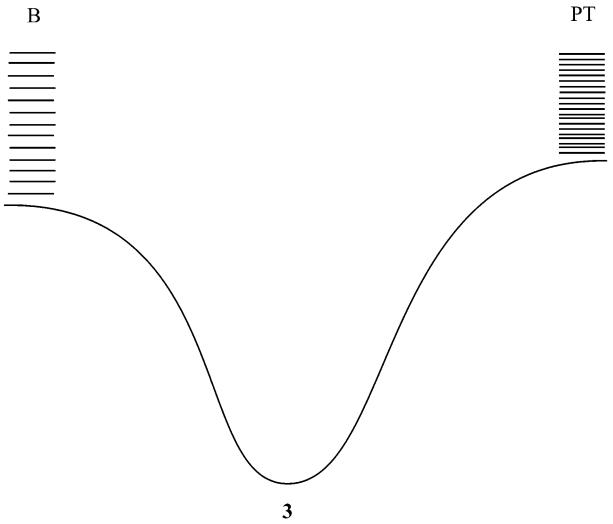

Figure 3. Potential energy surface for the reaction of $CH_3SOCH_3 + F^-$.

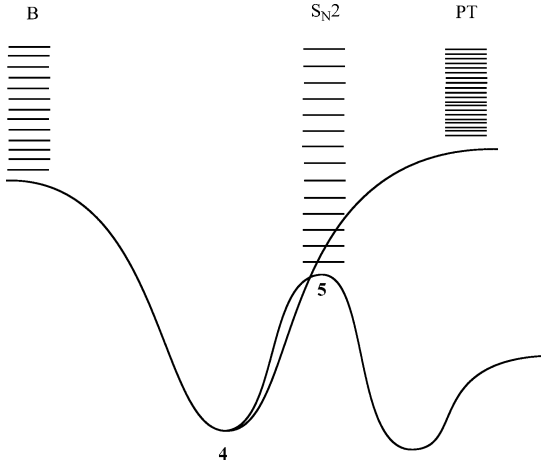

Figure 4. Potential energy surface for the reaction of $CH_3S(BH_3)CH_3 + F^-$.

channel) or dissociating back to the reactants (the B channel). The PT channel has a higher energy, but a higher density of quantum states above the transition state. The higher density of states is mainly the result of the increase in rotational degrees of freedom (increase in rotational entropy), from the atomic ion F^- in the reactants to the diatomic molecule H−F in the products.

The proton-transfer efficiency is determined by the competition between the B and the PT channels. The observed efficiency of 0.035 at 350 K means that about 3.5% of the collision complex reacts via the PT channel, while the majority of the complex dissociates back to reactants. The low efficiency of this reaction suggests that most of the collisions have an energy below the critical energy of the PT channel at 350 K. If we assume that the reactants have a Boltzmann distribution of energy upon collision, then about 4% of the collisions would surmount the 2.2 kcal/mol of endothermicity at 350 K. This is comparable to the observed efficiency of 3.5% at 350 K.

The observed rate constants as a function of increase in F^- translational energy in Figure 1 reflect the dynamic change of the efficiency at different energies. The PT channel is statistically favored at higher energies, because of the higher density of states at the transition state. A graphical description of density of states (shown as sum of states) versus total energy for the two dissociation channels of the PT intermediate complex is similar to that of dissociation of $[(NC)_2CH_2{\cdot}Cl]^-$.[38] With increasing system energy, more and more collision complexes will dissociate via the PT channel. As a result, the efficiency becomes larger at higher energies. Because the collision rate constants decrease slowly with increasing collision energy, the change of the observed rate constant will mainly be determined by the change of efficiency. Positive energy dependence for the overall proton-transfer reaction is expected. Indeed, we observed larger rate constants at higher F^- translational energies (Figure 1).

On the basis of studies with high-pressure mass spectrometry, Sieck and Mautner[13] suggested that fast bimolecular reactions can be characterized by a single well potential, so that $\Phi = K/(1 + K)$ and $\Phi_f + \Phi_r = 1$, where Φ is the efficiency (Φ_f, forward reaction, and Φ_r, reverse reaction) and K is the equilibrium constant.[12,13,39−42] Because K is finite, the efficiency in either direction alone cannot be unity. This elegant analysis assumed both a single well potential and also that the collision rate constants for the forward and back reactions were the same, which was quite reasonable given the reactions under consideration. For complex reactions, however, in which the entropy changes are large, even if the reaction proceeds on a single well potential, the collision rate constants may not be same for the forward and back reactions. Thus, both the collision rates and the efficiencies must be taken into account in understanding the rate constants.

The reaction of F^- with **2** has two competing channels, proton transfer and S_N2. The potential energy surface for the proton-transfer reaction has features similar to those for reaction 5, with a deep single well of 31 kcal/mol connected to the entrance (B) and the exit (PT) channels (Figure 4). The intermediate complex (**4**) associated with the well also has features similar to that of **3**, where a hydrogen-bonding interaction is involved in stabilizing the complex. The PT channel is about 2 kcal/mol higher than the B channel. In addition, a double well potential energy surface is employed to describe the S_N2 reaction. Stable structures, **4** and $[(CH_3SBH_3^-)CH_3F]$, associated with the two wells were determined from quantum calculations, and a S_N2 transition state structure (**5**) was located along the reaction path from complex **4** to $[(CH_3SBH_3^-)CH_3F]$. The S_N2 reaction shares the same entrance channel (B) and intermediate complex (**4**) with the proton-transfer reaction. Because the S_N2 reaction is highly exothermic (20 kcal/mol), the reactivity is mainly determined by the first well. The ion−molecule complex (**4**) can exit the well via three pathways, dissociation back to the reactants (B), formation of the proton-transfer products (PT), and crossing the S_N2 barrier (S_N2). Among the three pathways, the PT channel has the highest energy and also the highest density of quantum states. The high density of states is mainly due to the formation of H−F from F^-, which increases the rotational entropy. The S_N2 channel has the lowest energy and also the lowest density of states.

The efficiencies for the S_N2 and the proton-transfer reactions are determined by the competition among the three pathways

(42) Blondel, C.; Delsart, C.; Goldfarb, F. *J. Phys. B.: At. Mol. Opt. Phys.* **2001**, *34*, L281−L288.

(eqs 8, 9). The efficiencies observed at 350 K show that about 18% of the collision complexes dissociate via the S_N2 channel, and about 3% via the PT channel. The majority of the complexes (79%) dissociate back to the reactants. The low efficiency observed for the proton-transfer reaction suggests that a small fraction of the collisions occur above the critical energy of the PT channel, and most of the collisions occur at or below the PT channel. The S_N2 channel has the lowest critical energy, but is least favored entropically. It is not surprising that only about 18% of the collisions lead to the S_N2 products, although the S_N2 channel is about 7 kcal/mol lower than the B channel. The efficiency observed for the S_N2 reaction is comparable to that for the reaction of $Cl^- + NCCO_2CH_3$ giving $NCCO_2^- + CH_3Cl$.[26] The latter reaction has an efficiency of 0.19 and a potential energy surface with the central barrier 6.3 kcal/mol below the separated reactants. According to eqs 8 and 9, if k_{PT} is very small, the forward reaction would be dominated by the S_N2 channel, and the overall efficiency ($\Phi_{SN2} + \Phi_{PT}$) would be determined by Φ_{SN2}. In fact, we observed the overall efficiency of 0.21 as compared to 0.18 for the S_N2 reaction at 350 K.

The relative densities of states associated with the three pathways connected to the well associated to **4** determine the dynamic changes of the microscopic rate constants and efficiencies. With increasing system energy, the changes of microscopic rate constants would be in the order of $\Delta k_{PT} > \Delta k_B > \Delta k_{SN2}$. The efficiencies for the PT channel would increase, and for the S_N2 channel they would decrease. Similar to reaction 5, the collision rate constant for F^- with **2** decreases slowly with increasing collision energy. Therefore, changes of the observed rate constants would be determined by efficiencies. Positive energy dependence is expected for the proton-transfer reaction, and negative energy dependence is expected for the S_N2 reaction. We indeed observed the increase in proton-transfer rate constants and the decrease in S_N2 rate constants at higher F^- translational energy (Figure 2).

Can we expect 100% proton-transfer products at even higher energy? Using an analysis similar to that applied to reaction 5, there is always a nonzero fraction of collisions whose total energy is below the critical energy of the PT channel under thermal condition. This fraction of collisions does not have enough energy to access the PT channel. Therefore, the endothermic proton-transfer reaction must have less than unit efficiency and less than 100% product branching ratio. The experimentally observed overall rate constants appear to be insensitive to energy change. This may be due to the fact that the S_N2 and the proton-transfer reactions have opposite effects on the overall rate constants, and the effects happen to have similar magnitudes within the energy range examined.

Statistical modeling shows that the observed proton-transfer rate constants in reaction 5 agree with RRKM theory predictions (Figure 1). The apparent statistical behavior may be due to the strong binding energy of the complex, which results in a longer lifetime of the complex for statistical redistribution of the additional kinetic energy. For reaction 6, the observed overall rate constants agree with RRKM calculations, and both the S_N2 and the proton-transfer reactions agree with theory within an additional 2.5 kcal/mol of kinetic energy (Figure 2). The agreement between experiment and theory is consistent with the statistical partitioning of the additional kinetic energy, which may also result from the relatively long lifetime of the intermediate complex. For the S_N2 reaction to occur, complex **4** has to rearrange to a S_N2 reactant complex with a backside orientation of the F^- relative to the leaving group, just like that in $[(NC)_2CH_2 \cdot Cl]^-$ system.[38] The lifetime of the complex has to be long enough for this rearrangement. At higher energy, theory predicts a larger difference of the rate constants between the PT and the S_N2 channels. This may be due to the choice of the frequencies in the transition states and the use of an approximate statistical model; that is, an effective temperature is used based on the total system energy.

Conclusion

We have investigated the dynamics of an endothermic proton-transfer reaction of F^- with dimethyl sulfoxide and a competitive reaction system of F^- with borane-methyl sulfide complex, an endothermic proton transfer competing with an exothermic S_N2 channel. We measured rate constants as a function of F^- translational energy and modeled reaction kinetics with RRKM theory. Both proton-transfer reactions have positive entropy changes in the forward directions and show positive kinetic energy dependences. The competing S_N2 reaction shows negative energy dependence and becomes less important at higher energies. The observed kinetics agree with RRKM theory predictions within a few kcal/mol of additional kinetic energies. Dynamic analysis indicates that an endothermic reaction must have less than unit efficiency and must be slower than the collision rate at thermal condition, even though the reaction has an overall negative free energy change. The branching ratio for the two competing channels results from the competition of a combined factor of relative critical energy and density of states. The changes of the branching ratio as a function of system energy reflect the dynamic change of the microscopic rate constants associated with each channel.

Acknowledgment. We are grateful to the National Science Foundation for support of this work.

JA030006Z